



Supplement of

Optical properties of atmospheric fine particles near Beijing during the HOPE-J³A Campaign

X. Xu et al.

Correspondence to: W. Zhao (wxzhao@aiofm.ac.cn) and W. Zhang (wjzhang@aiofm.ac.cn)

The copyright of individual parts of the supplement might differ from the CC-BY 3.0 licence.

30 **S1 Mass extinction efficiencies of each chemical composition at different**
31 **wavelength**

32

33 The mass extinction efficiencies (MEE) for a single sphere particle can be calculated by
34 using Mie theory (Bohren and Huffman, 1998):

35
$$MEE = \frac{3Q_{ext}(m, D_p, \lambda)}{2\rho D_p} \quad (1)$$

36 where $m = n + ik$ is the complex refractive index (CRI) of the particle (n and k
37 corresponding to the real and imaginary parts of the CRI, respectively), D_p is the mean
38 diameter per unit volume, λ is the incident light wavelength, and ρ is the density of the
39 particle.

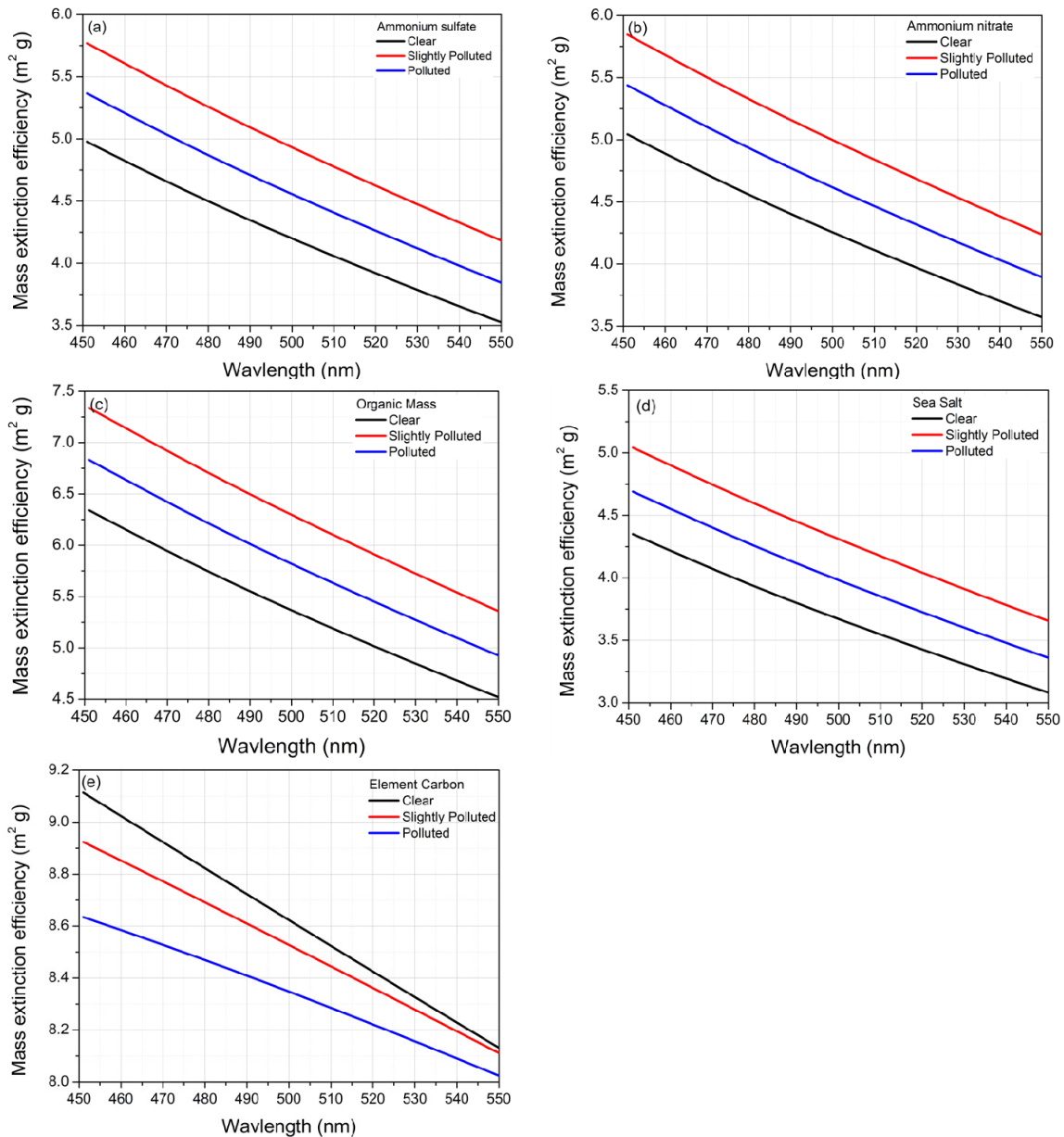
40 The MEE of each chemical composition can be calculated by using Mie algorithm with
41 the measured volume size distributions and with an assumed CRI of each compound, as
42 shown in equation (2) (Cheng et al., 2008; Cheng et al., 2015):

43
$$MEE(j) = \frac{\sum_{bin=1}^{D_{bin}} MEE(j, D_{bin}) V_{j,bin}}{\sum_{bin=1}^{D_{bin}} V_{j,bin}} \quad (2)$$

44 where $MEE(j, D_{bin})$ is the j th component of MEE in the size bin (D_{bin}), which can be
45 calculated using equation (1). $\sum_{bin=1}^{D_{bin}} V_{j,bin}$ is the volume size distribution and $V_{j,bin}$ is the
46 volume concentration.

47 In this study, since size-segregated chemical composition was not available, the
48 following method was used to calculate the MEE of each composition. We assumed that the
49 particles were external mixed and each chemical components were uniformly distributed, and
50 we also assumed that the CRIs do not vary with the wavelength. The densities and CRIs of
51 different types of aerosols were shown in Table S1 (Cheng et al., 2008). The size-distribution
52 of each component (organic mass, ammonium nitrate, ammonium sulfate, sea salt, and
53 element carbon) was calculated by the volume size distribution (observed data from Scanning
54 Mobility Particle Sizer Spectrometer (SMPS)) and the mass concentrations. Thus, the

55 wavelength-dependent *MEE* of each component can be calculated by equation (1) and (2).
 56 Fig.S1 shows the values of *MEEs* decreased with increasing light incident wavelength, and
 57 depended on the air pollution levels. As an average result, the calculated dry mass extinction
 58 efficiencies of inorganic mass (including sulfate, nitrate and sea salt), organic mass and
 59 element carbon at $\lambda = 470$ nm were 1.31, 1.30 and 1.08 times larger than that at $\lambda = 550$ nm.
 60



61
 62 Fig. S1 Calculated wavelength dependent mass extinction efficiencies of inorganic mass
 63 (including sulfate, nitrate and sea salt), organic mass and element carbon.

64
 65

66 Table S1 Densities and complex refractive indexes of different types of aerosols. (adapted
 67 from Cheng et al., 2008)

Chemical Species	Density (g cm ⁻³)	Complex Refractive Index
(NH ₄) ₂ SO ₄	1.748	1.54 - 10 ⁻⁷ i
NH ₄ NO ₃	1.725	1.54 - 10 ⁻⁷ i
OM	1.4	1.55 - 0.001 i
Sea salt	2.0	1.54 - 10 ⁻⁷ i
EC	1.5	1.80 - 0.54 i

70

71

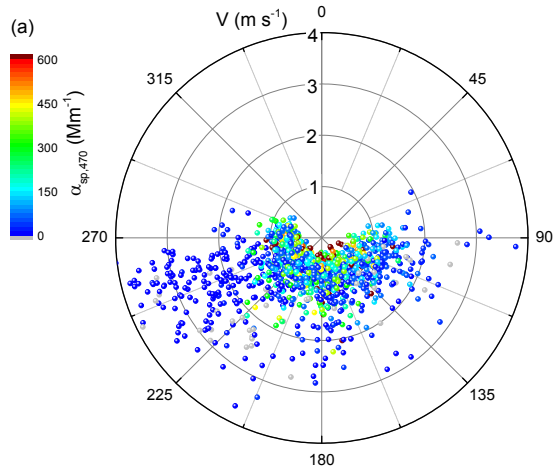
72 S2 Relationships between aerosol optical properties and wind directions

73

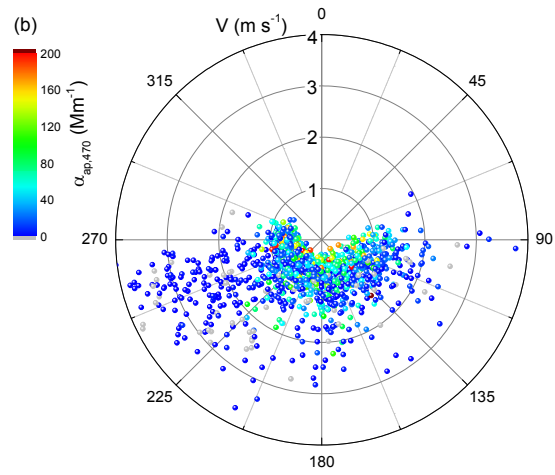
74 The local wind direction and wind speed were measured on the roof of building with a
 75 Gill MetPak- II weather station. Fig. S2 presents the relationship of $\alpha_{sp,470}$, $\alpha_{ap,470}$ and ω_{470} to
 76 local wind directions and wind speed during the campaign. On these graphs, Beijing centre
 77 would be at $\sim 206^\circ$. Fig. S2a and S2b display the wind direction versus wind speed, with
 78 $\alpha_{sp,470}$ and $\alpha_{ap,470}$ as the color scale. From November 2014 to January 2015, the winds were
 79 mostly from the southeast and southwest. There was no obvious correlation between
 80 extensive optical properties and wind direction. The average wind speed was 1.2 m s⁻¹ during
 81 the field campaign. When the instantaneous wind speeds were higher than the average wind
 82 speed, the values of $\alpha_{sp,470}$ and $\alpha_{ap,470}$ decreased. The average values of $\alpha_{sp,470}$ for $v < 1.2$ m
 83 s⁻¹ and $v > 1.2$ m s⁻¹ were 198 Mm⁻¹ and 54 Mm⁻¹, respectively. Similarly, the average values
 84 of $\alpha_{ap,470}$ for $v < 1.2$ m s⁻¹ and $v > 1.2$ m s⁻¹ were 41 Mm⁻¹ and 11 Mm⁻¹, respectively. When $v >$
 85 1.2 m s⁻¹, lower values of $\alpha_{sp,470}$ (< 100 Mm⁻¹) and $\alpha_{ap,470}$ (< 50 Mm⁻¹) occurred more
 86 frequently when the local wind came from 225 - 270°, which indicated that the air parcel was
 87 relatively clean in the wind direction. When $v < 1.2$ m s⁻¹, values of $\alpha_{sp,470}$ and $\alpha_{ap,470}$
 88 occurred similar frequently and ranged widely when the local wind same from the south. Fig.
 89 S2c shows the relationship between the wind direction and ω_{470} , with the color scale as wind
 90 speed. The average value of ω_{470} ranged from 0.7 to 0.9 and was not strongly correlated with
 91 the wind direction. However, higher values ω_{470} (0.9 - 1.0) occurred more frequently when
 92 the local wind came from 270 - 160°, which indicated that the air parcel in this wind direction
 93 contained less light absorbing particulate matter.

94

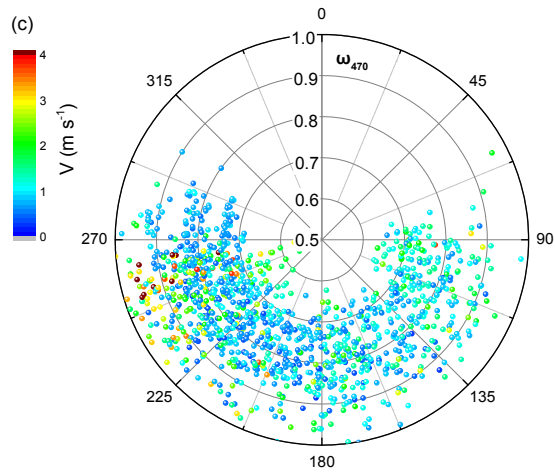
95



96



97



98

99 Fig. S2 Local wind direction and wind speed plots for the campaign: (a) wind direction
 100 versus wind speed (m s^{-1}), with $\alpha_{sp,470}$ (Mm^{-1}) as the color scale, (b) wind direction versus
 101 wind speed (m s^{-1}), with $\alpha_{ap,470}$ (Mm^{-1}) as the color scale, and (c) wind direction versus ω_{470} ,
 102 with the color scale as wind speed (m s^{-1}).
 103
 104

105

106 **References**

107

108 Bohren, C. F., and Huffman, D. R. : Absorption and Scattering of Light by Small Particles;
109 John Wiley & Sons: New York, 1998.

110 Cheng, Y. F., Wiedensohler, A., Eichler, H., Su, H., Gnauk, T., Brüggemann, E., Herrmann, H.,
111 Heintzenberg, J., Slanina, J., Tuch, T., Hu, M., and Zhang, Y. H.: Aerosol optical
112 properties and related chemical apportionment at Xinken in Pearl River Delta of China,
113 Atmos. Environ., 42, 6351-6372, doi: 10.1016/j.atmosenv.2008.02.034, 2008.

114 Cheng, Z., Jiang, J., Chen, C., Gao, J., Wang, S., Watson, J. G., Wang, H., Deng, J., Wang, B.,
115 Zhou, M., Chow, J. C., Pitchford, M. L., and Hao, J.: Estimation of aerosol mass
116 scattering efficiencies under high mass loading: case study for the megacity of
117 Shanghai, China, Environ. Sci. Tech., 49, 831-838, 10.1021/es504567q, 2015.

118